



Synthesis, silver (I) extraction and silver (I) binding studies of novel N^1, N^3 -bis(2-(benzylthio)ethyl)propanediamide derivatives

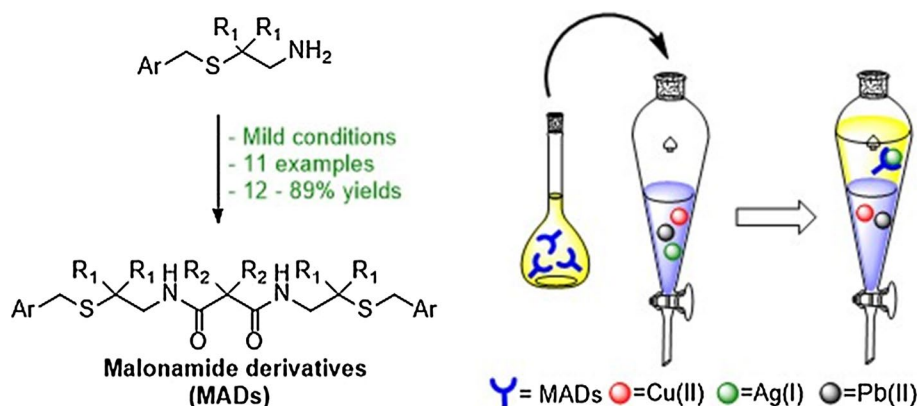
Abiodun D. Aderibigbe^{1,2} · Andrew J. Clark¹

Received: 21 May 2020 / Accepted: 6 August 2020
© Institute of Chemistry, Slovak Academy of Sciences 2020

Abstract

Solvent or liquid–liquid extraction represents a highly valuable technique for the selective recovery of metals from the aqueous phase due to the ease of operation and short turnaround times. Ligands bearing soft donor atoms including nitrogen and sulfur are ideal candidates for selective silver recovery due to their preference for silver binding. Herein, novel N^1, N^3 -bis(2-(benzylthio)ethyl)propanediamide derivatives bearing sulfur and nitrogen donor atoms were prepared in low to high yields and tested for Ag^+ extraction from ternary aqueous solutions also containing Cu^{2+} and Pb^{2+} following a well-established solvent extraction protocol. It was observed that electronics effects at the 4-aryl position in the propanediamide (or malon-diamide) derivatives had a significant effect on the selectivity, but little effect on the efficiency of Ag^+ extraction with the 4-methoxy analogue proving the most selective. Steric hindrance provided by dimethyl substitutions at the α -positions to the sulfur atoms had negative effects on Ag^+ extraction efficiency and selectivity, while diethyl steric hindrance at the methylene center lowered selectivity but increased extraction efficiency for Ag^+ . Detailed binding studies reveal that one of the malondiamide derivatives which lacked the electronic and steric hindrance groups studied coordinated Ag^+ in a 1:1 fashion suggesting a tetrahedral complex geometry. Overall, the results show that simple modification of the electronics and sterics of the N^1, N^3 -bis(2-(benzylthio)ethyl)propanediamides, can improve their selectivity for Ag^+ recovery from the aqueous phase.

Graphic abstract



Keywords Malondiamide derivatives · Selective silver(I) extraction · Electronics · Sterics · Job plot · ¹H NMR titration

Electronic supplementary material The online version of this article (<https://doi.org/10.1007/s11696-020-01307-x>) contains supplementary material, which is available to authorized users.

✉ Abiodun D. Aderibigbe
abiodunadaderibigbe23@gmail.com

Extended author information available on the last page of the article

Introduction

As the world population increases, the demand for products like phones, laptops, batteries and jewelry, containing precious metals like silver is certain to increase as well

(Taillades and Sarradin 2004; Sahan et al. 2019). Unfortunately, silver just like other metals is a non-renewable resource. Therefore, to meet the increasing demand, the supply of silver must be guaranteed. Two major options that have been explored to guarantee the supply of silver and indeed other metals is the search for new primary sources or new metal ore deposits (Kolpakova et al. 2019), and the secondary sources or urban mining, in other words, recycling of metals (Avarmaa et al. 2019). The success of these options rests on the development of an efficient, metal selective and cost-effective Ag^+ recovery process.

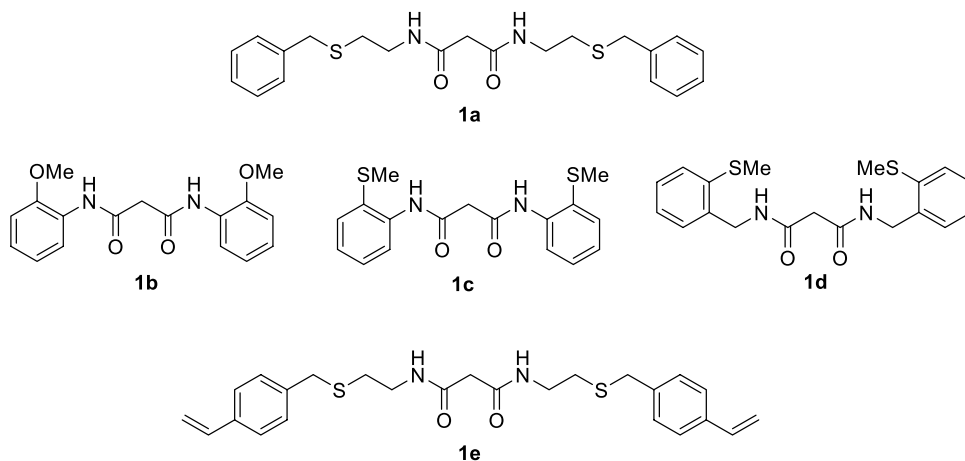
To date, a considerable number of studies have reported on the recovery of Ag^+ by membrane filtration (Zanain and Lovitt 2013), ion exchange (Virolainen et al. 2015), electrochemical treatment (Ölmez 2009; Selim et al. 2017), solid phase extraction/adsorption (Chen and Wang 2008; El-Shafey and Al-Kindy 2013; Aderibigbe et al. 2020) and solvent extraction (Saha et al. 2013; Bray et al. 2015). Solvent extraction is a popular technique due to the ease of operation, low operating costs, short turnaround times and the ability of extractants to form stable complexes with the metal ion (Nishihama et al. 2001; Grigorieva et al. 2018). Extractants containing at least one of phosphorus, nitrogen or sulfur donor atoms have been reported to be selective for the extraction of Ag^+ from the aqueous phase consistent with the hard/soft acid/base rule (Pearson 1968; Alam et al. 1997; Ohto et al. 1997; Shimojo and Goto 2004; Saha et al. 2013). For example, Bray et al. (2015) reported that the ligand—1,3,5-tris((pyridin-4-ylthio)methyl)benzene bearing sulfur donors demonstrated better efficiency and selectivity for Ag^+ compared with other ligands containing oxygen donors. In a different study, an oxime-based extractant (LIX63) containing a nitrogen donor was found to selectively extract Ag^+ over Zn^{2+} , achieving extraction efficiencies of 60% and 0% for Ag^+ and Zn^{2+} , respectively, from the aqueous phase. The extracted Ag^+ was later stripped from the LIX63 extractant using aqueous ammonia also containing a nitrogen donor

(Sun et al. 2017). Furthermore, the disulphide extractant—bis(2,4,4-trimethylpentyl)dithiophosphinic acid-containing sulfur and phosphorus donors was reported to demonstrate remarkable selectivity for Ag^+ from a chloride solution containing more than 1000-fold excess of other transition metals. Extraction efficiencies of 98.6, 0.2, 0.6, 0.6 0.5 and 0.7% were observed for Ag^+ , Ni^{2+} , Cu^{2+} , Co^{2+} , Zn^{2+} and Fe^{3+} , respectively. The loaded extractant was completely stripped of Ag^+ using a 0.5 M thiourea solution containing a sulfur donor (Grigorieva et al. 2018).

N^1, N^3 -propanediamide or malondiamide derivatives (MADs) such as **1a** (Fig. 1) have attracted attention due to their versatility for metal recovery in separation science, having demonstrated outstanding efficiency and selectivity in the recovery of highly valuable metals including lanthanides, actinides and precious metals (Daubinet and Kaye 2002; Manchanda and Pathak 2004; Jańczewski et al. 2007; Patil et al. 2014). The presence of two acyl groups and an active methylene center allows for the modification of the structural features of the MADs towards accessing derivatives with selective metal recovery and desired solubility properties (Daubinet and Kaye 2002). Addition of specific donors has been shown to improve the efficiency and selectivity of the MADs for metal recovery. For example, Daubinet and Kaye (2002) prepared a range of MADs (**1a–d**) (Fig. 1) with different donor groups and varying degrees of lipophilicities via a microwave-assisted method and observed that the MAD **1a** bearing a benzylthio arm demonstrated the highest efficiency (97%) and selectivity for Ag^+ recovery from aqueous solution also containing Cu^{2+} and Pb^{2+} .

As part of an ongoing research project exploring the development of technologies for recovery of Ag^+ from waste repositories (including metallurgical slag heaps, mine tailings and possibly landfills), we queried the possibility of accessing a Ag^+ -selective ligand bearing a vinyl handle which can be tethered by polymerization to a magnetic nanoparticle. The MAD **1e**, (Fig. 1) was

Fig. 1 N^1, N^3 -bis(2-(benzylthio)ethyl)propanediamide derivatives **1a–e**



chosen as our initial target after we had judged that it could be easily prepared and that it has high stability in low pH environments. Unfortunately, previously reported conditions for accessing the related ligand **1a** involve high temperatures which we feared could occasion the polymerization of the important vinyl group in **1e** (Daubinet and Kaye 2002). Therefore, initial study focused on the development of a room temperature synthetic route to accessing derivatives of **1a**; **1e–i** (Fig. 2). Subsequently structure–activity relationship of the synthesized ligands (**1a**, **1e–i**), in particular the effect of electronics (using **1a** and **1e–h**) and sterics (using **1a**, **1i** and **3a**) (Fig. 2) on Ag^+ extraction was investigated to understand how modification affects the selectivity and efficiency of the ligand. Finally, the binding stoichiometry of the Ag^+ -**1a** complex, as an example, was thoroughly investigated to gain an insight into the Ag^+ binding nature of the N^1, N^3 -bis(2-(benzylthio)ethyl)propanediamide derivatives prepared in this study.

Experimental details

Chemicals and instrumentation

All reagents were purchased from commercial sources (Sigma Aldrich, VWR, Alfa Aesar and Acros Organics) and used as received. Proton (^1H) and Carbon-13 (^{13}C) NMR spectra were recorded at room temperature on Bruker Advance spectrometers and all chemical shift values were referenced to an internal standard of tetramethylsilane ($\delta = 0.0$ ppm). Fourier transform infra-red (FTIR) spectra were recorded on Bruker Alpha Platinum-Attenuated Total Reflectance IR spectrometer. All mass spectra were run on a Bruker MaXis mass spectrometer. Metal concentrations were measured by means of a PerkinElmer 5300DV Inductively Coupled Plasma Optical Emission spectrophotometer (ICP-OES).

Methods

General synthesis procedure for the 2-(benzylthio)ethan-1-amine derivatives (**2a–e**)

The 2-(benzylthio)ethan-1-amine derivatives **2a–e** were synthesized following the method reported by Ghosh and Tochtrop (2009). Briefly, to a stirred H_2O /ethanol (1:3) solution of LiOH (2 eq.) and 2-aminoethanethiol hydrochloride (1 eq.) was added dropwise for 5 min, the appropriate benzyl chlorides (1 eq.) and the reaction was left to stir at 35°C for 20 min (for **2a**) or 40 min (for **2b–e**) after which the solvent was removed in vacuo. The crude mixture was extracted with dichloromethane (DCM) after it had been solubilized with H_2O . The DCM extract was then dried with anhydrous Na_2SO_4 or MgSO_4 , filtered and concentrated in vacuo. All amines except for **2d** (the fluoro analogue) were obtained as oils needing no purification. The amine **2d** was subsequently purified by column chromatography using a mobile phase gradient of 100% EtOAc to 50% v/v EtOAc/MeOH.

2-(Benzylthio)ethan-1-amine (2a) (Ghosh and Tochtrop 2009) Viscous colorless oil. Yield: 5.76 g (86%), $\nu(\text{cm}^{-1})$ 3363, 3279 (N–H stretch), 1600 (N–H bend), ^1H NMR (400 MHz, CDCl_3) δ 7.39 – 7.18 (m, 5H, ArH), 3.70 (s, 2H, PhCH_2S), 2.81 (t, $J = 6.5$ Hz, 2H, SCH_2CH_2), 2.51 (t, $J = 6.5$ Hz, 2H, SCH_2CH_2), 1.29 (s, 2H, $\text{CH}_2\text{CH}_2\text{NH}_2$), ^{13}C NMR (100 MHz, CDCl_3) 138.5, 128.9, 128.6 and 127.1 (ArC), 40.9 ($\text{CH}_2\text{CH}_2\text{NH}_2$), 36.0 (PhCH_2S), 35.7 (SCH_2CH_2); m/z (ESI): 168 $[\text{M} + \text{H}]^+$.

2-((4-Vinylbenzyl)thio)ethan-1-amine (2b) Viscous yellow oil. Yield: 5.87 g (77%), $\nu(\text{cm}^{-1})$ 3365, (N–H stretch), 1627, 1567 (N–H bend), ^1H NMR (300 MHz, CDCl_3) δ 7.36 (d, $J = 8.0$ Hz, 2H, ArH), 7.27 (d, $J = 8.0$ Hz, 2H, ArH), 6.70 (dd, $J = 17.5, 11.0$ Hz, 1H, CH_2CHPh), 5.73 (d, $J = 17.5$ Hz, 1H, $\text{CH}_a\text{H}_b\text{CHPh}$), 5.23 (d, $J = 11.0$ Hz, 1H, $\text{CH}_a\text{H}_b\text{CHPh}$), 3.69 (s, 2H, PhCH_2S), 2.82 (t, $J = 6.0$ Hz, 2H, $\text{CH}_2\text{CH}_2\text{NH}_2$), 2.51 (t, $J = 6.0$ Hz, 2H, SCH_2CH_2), 1.29 (s, 2H, $\text{CH}_2\text{CH}_2\text{NH}_2$), ^{13}C NMR (75 MHz, CDCl_3) δ 138.1

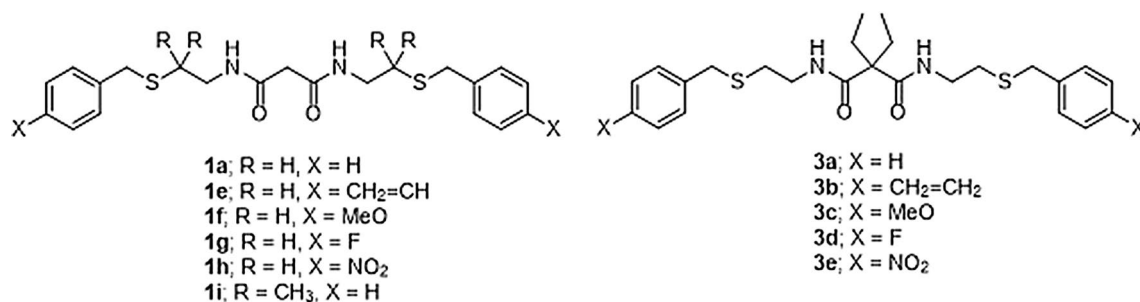


Fig. 2 N^1, N^3 -bis(2-(benzylthio)ethyl)propanediamide derivatives synthesized in this study

and 136.5 (ArC), 136.4 (CH_2CHPh), 129.1 and 126.5 (ArC), 113.9 (CH_2CHPh), 41.0 ($\text{CH}_2\text{CH}_2\text{NH}_2$), 35.8 (PhCH_2S), 35.7 (SCH_2CH_2), m/z (ESI): $[\text{M} + \text{H}]^+$ for $[\text{C}_{11}\text{H}_{16}\text{NS}]^+$, calculated; 194.1003, found 194.0998.

2-((4-Methoxybenzyl)thio)ethan-1-amine (2c) (Ghosh and Tochtrop 2009) Viscous colorless oil. Yield: 4.37 g (88%), $\nu(\text{cm}^{-1})$: 3261 (N–H stretch), 1663 (N–H bend), ^1H NMR (400 MHz, CDCl_3) δ 7.23 (d, $J=8.5$ Hz, 2H) and 6.84 (d, $J=8.5$ Hz, 2H) (ArH), 3.79 (s, 3H, CH_3OPh), 3.67 (s, 2H, PhCH_2S), 2.85 (t, $J=6.5$ Hz, 2H, $\text{CH}_2\text{CH}_2\text{NH}_2$), 2.71 (s, 2H, $\text{CH}_2\text{CH}_2\text{NH}_2$), 2.55 (t, $J=6.5$ Hz, 2H, SCH_2CH_2). ^{13}C NMR (100 MHz, CDCl_3) δ 159.0, 130.2, 130.0 and 114.1 (ArC), 55.4 (CH_3OPh), 40.5 ($\text{CH}_2\text{CH}_2\text{NH}_2$), 35.4 (PhCH_2S), 34.5 (SCH_2CH_2), m/z (ESI): 198 $[\text{M} + \text{H}]^+$.

2-((4-Fluorobenzyl)thio)ethan-1-amine (2d) (Ghosh and Tochtrop 2009) Viscous colorless oil. Yield: 4.27 g (85%), $\nu(\text{cm}^{-1})$: 3365 (N–H stretch), 1599 (N–H bend), ^1H NMR (400 MHz, CDCl_3) δ 7.35–7.23 (dd, 2H, $J_{\text{HCCCH}}=9$ Hz, $J_{\text{HCCCH}}=3$ Hz, ArH), 7.06–6.96 (t, 2H, $J_{\text{HCCF}}=15$ Hz, ArH), 3.68 (s, 2H, PhCH_2S), 2.82 (t, $J=6.5$ Hz, 2H, $\text{CH}_2\text{CH}_2\text{NH}_2$), 2.51 (t, $J=6.5$ Hz, 2H, SCH_2CH_2), 1.33 (s, 2H, $\text{CH}_2\text{CH}_2\text{NH}_2$), ^{13}C NMR (100 MHz, CDCl_3) δ 162 (d, $J_{\text{CF}}=244$ Hz), 134.2 (d, $J_{\text{CCCCF}}=3$ Hz), 130.4 (d, $J_{\text{CCF}}=8$ Hz) and 115.4 (d, $J_{\text{CCF}}=21$ Hz) (ArC), 40.9 ($\text{CH}_2\text{CH}_2\text{NH}_2$), 35.6 (PhCH_2S), 35.2 (SCH_2CH_2), m/z (ESI): 186 $[\text{M} + \text{H}]^+$.

2-((4-Nitrobenzyl)thio)ethan-1-amine (2e) (Ghosh and Tochtrop 2009) Yellow oil. Yield: 3.23 g (85%), $\nu(\text{cm}^{-1})$: 3365 (N–H stretch), 1599 (N–H bend), 1367 (N–O stretch), ^1H NMR (300 MHz, CDCl_3) δ 8.18 (d, $J=8.5$ Hz, 2H, ArH), 7.50 (d, $J=8.5$ Hz, 2H, ArH), 3.79 (s, 2H, PhCH_2S), 2.85 (t, $J=6.5$ Hz, 2H, $\text{CH}_2\text{CH}_2\text{NH}_2$), 2.53 (t, $J=6.5$ Hz, 2H, SCH_2CH_2), 1.38 (s, 2H, $\text{CH}_2\text{CH}_2\text{NH}_2$), ^{13}C NMR (75 MHz, CDCl_3) δ 147.1 (ArC), 146.4 (ArC), 129.7 (ArC), 123.9 (ArC), 40.9 ($\text{CH}_2\text{CH}_2\text{NH}_2$), 35.8 (PhCH_2S), 35.6 (SCH_2CH_2), m/z (ESI): 213 $[\text{M} + \text{H}]^+$.

Synthesis of 2,2-dimethyl-2-benzylthioethylamine (2g)

Access to 2,2-dimethyl-2-benzylthioethylamine **2g** was gained following the method reported by Carroll et al. (1963). In the first step, a mixture of acetone (3.67 mL, 0.05 mol), benzylmercaptan (5.90 mL, 0.05 mol), nitromethane (2.71 mL, 0.05 mol) and benzene (18.75 mL) were heated at 100 °C inside a flask fitted with a Dean Stark apparatus filled with benzene. After 22 h, the crude mixture still in the benzene solvent was left to cool to room temperature, transferred into a separatory funnel where it was washed with 2.0 M HCl (20 mL \times 2) and then with H_2O (20 mL \times 2). It was then dried with anhydrous MgSO_4 ,

concentrated in vacuo and purified by flash chromatography using *n*-hexane as eluent to yield 1-(benzylthio)-1,1-dimethylnitroethane **2f** (2.60 g, 23%). In the second step, a dry ether solution of 1-(benzylthio)-1,1-dimethylnitroethane **2f** (1 g, 4.4 mmol) was added to a cold ether solution of LiAlH_4 (4 M, 3.25 mL) inside a two-necked flask. The mixture was left to stir for another 3 min after which it was transferred to a heating block and heated under reflux for 100 min. The crude mixture was transferred to a 250 mL flask and a stir bar added. H_2O and subsequently potassium sodium tartarate (25 mL, 20% w/w) was added. The mixture was left to stir until all solids dissolved. The crude product was then extracted with ether (20 mL \times 3) and purified by flash chromatography (16 – 50% ethyl acetate: *n*-hexane, ethyl acetate and finally methanol) to furnish 2-(benzylthio)-2,2-dimethylmethylethylamine **2g** as a yellow oil. Yield: (0.60 g, 70%), $\nu(\text{cm}^{-1})$ 3376 (NH), ^1H (300 MHz CDCl_3) 7.40–7.19 (m, 5H, ArH), 3.68 (s, 2H, PhCH_2S), 2.61 (s, 2H, CH_2NH_2), 1.44 (s, 2H, NH_2), 1.28 (s, 6H, $\text{SC}(\text{CH}_3)_2$); ^{13}C (75 MHz, CDCl_3) 138.5, 129.0, 128.7 and 127.1 (ArC), 51.8 ($\text{C}(\text{CH}_3)_2\text{CH}_2\text{NH}_2$), 48.9 ($\text{C}(\text{CH}_3)_2\text{CH}_2\text{NH}_2$), 32.8 (PhCH_2S), 26.6 ($\text{C}(\text{CH}_3)_2\text{CH}_2\text{NO}_2$), m/z (ESI): 196 $[\text{M} + \text{H}]^+$.

General synthesis procedure for the N^1, N^3 -bis(2-(benzylthio)ethyl)propanediamide derivatives (1a and 1e-i)

To a stirred solution of the amines **2a–e**, **2g** (1 eq.) in dry THF, malonyl chloride (0.25 eq.) solution in dry THF was added dropwise for 90 min. The reaction mixture was left to stir overnight and the THF solvent was removed in vacuo after which H_2O was added and the crude product was extracted with EtOAc. The EtOAc extracts were washed successively with HCl (2 M), saturated NaHCO_3 , H_2O and finally brine. It was then dried over Na_2SO_4 and concentrated in vacuo and purified by flash chromatography (20% EtOAc/Hexane to 100% EtOAc) to deliver the MADs **1a** and **1e–i**.

N^1, N^3 -bis(2-(benzylthio)ethyl)propanediamide (1a) Yellow powder. Yield: 0.21 g (33%), m.p.: 108–112 °C ((Daubinet and Kaye 2002): 105–106 °C), $\nu(\text{cm}^{-1})$: 3296 (amide N–H stretch), 1647 (amide C=O bend), ^1H NMR (400 MHz, CDCl_3) δ 7.40–7.19 (m, 10H, ArH), 7.05 (s, 2H, CONHCH_2), 3.71 (s, 4H, PhCH_2S), 3.39 (m, 4H, NHCH_2CH_2), 3.10 (s, 2H, COCH_2CO), 2.56 (t, $J=6.5$ Hz, 4H, $\text{CH}_2\text{CH}_2\text{S}$), ^{13}C NMR (100 MHz, CDCl_3) δ 167.3 (COCH_2CO), 138.2, 129.0, 128.8 and 127.3 (ArC), 43.1 (COCH_2CO), 38.5 (NHCH_2CH_2), 36.0 (PhCH_2S), 30.9 ($\text{CH}_2\text{CH}_2\text{S}$), m/z (ESI): 425 $[\text{M} + \text{Na}]^+$.

N^1, N^3 -bis(2-((4-vinylbenzyl)thio)ethyl)propanediamide (1e) Yellow powder. Yield: 0.09 g (33%), m.p.: 151–156 °C,

$\nu(\text{cm}^{-1})$: 3292 (amide N–H stretch), 1648 (amide C=O bend), $^1\text{H NMR}$ (400 MHz, CDCl_3) δ 7.36 (d, $J=7.5$ Hz, 4H) and 7.27 (d, $J=7.5$ Hz, 4H) (ArH), 6.94 (s, 2H, CONHCH₂), 6.69 (dd, $J=17.5, 11.0$ Hz, 2H, PhCH₂CH₂H_b), 5.73 (d, $J=17.5$ Hz, 2H, PhCH₂CH₂H_b), 5.24 (d, $J=11.0$ Hz, 2H, PhCH₂CH₂H_b), 3.70 (s, 4H, PhCH₂S), 3.40 (m, CH₂CH₂NH), 3.11 (s, 2H, COCH₂CO), 2.56 (t, $J=6.5$ Hz, 4H, SCH₂CH₂), $^{13}\text{C NMR}$ (100 MHz, CDCl_3) δ 167.2 (COCH₂CO), 137.7 and 136.8 (ArC), 136.5 (CH₂CHPh), 129.2 and 126.6 (ArC), 114.1 (PhCH₂CH₂), 43.1 (COCH₂CO), 38.4 (CH₂CH₂NH), 35.7 (CH₂SCH₂), 30.8 (SCH₂CH₂), m/z (ESI): $[\text{M} + \text{Na}]^+$ for $[\text{C}_{25}\text{H}_{27}\text{N}_2\text{NaO}_2\text{S}_2]^+$ calculated: 477.1646, found: 477.1643.

***N*¹,*N*³-bis(2-((4-methoxybenzyl)thio)ethyl)propanediamide (1f)** Yellow solid. Yield: 0.43 g (12%), m.p.: 146–149 °C., $\nu(\text{cm}^{-1})$: 3337 (NH), 1650 (amide C=O bend), 1240 (C–O; aromatic ether), $^1\text{H NMR}$ (300 MHz, CDCl_3) δ 7.24 (d, $J=8.5$ Hz, 4H, ArH), 6.97 (s, 2H, CH₂CH₂NH), 6.85 (d, $J=8.5$ Hz, 4H, ArH), 3.79 (s, 6H, CH₃Oph), 3.67 (s, 4H, PhCH₂S), 3.40 (m, 4H, CH₂CH₂NH), 3.11 (s, 2H, COCH₂CO), 2.55 (t, $J=6.5$ Hz, 4H, SCH₂CH₂), $^{13}\text{C NMR}$ (75 MHz, CDCl_3) δ 167.2 (COCH₂CO), 158.6 (ArC), 130.1 (ArC), 130.0 (ArC), 114.2 (ArC), 55.4 (CH₃O), 43.1 (COCH₂), 38.5 (CH₂CH₂NH), 35.4 (PhCH₂S), 30.8 (SCH₂CH₂), m/z (ESI): $[\text{M} + \text{Na}]^+$ for $[\text{C}_{23}\text{H}_{30}\text{N}_2\text{NaO}_4\text{S}_2]^+$ calculated: 485.1545, found: 485.1539.

***N*¹,*N*³-bis(2-((4-fluorobenzyl)thio)ethyl)propanediamide (1g)** Yellow powder. Yield: 0.55 g (31%), m.p.: 121–123 °C., $\nu(\text{cm}^{-1})$: 3296 (amide N–H), 1647 (amide C=O bend), $^1\text{H NMR}$ (400 MHz, CDCl_3) δ 7.28 (d, $J_{\text{HCCF}}=13.5$ Hz, 4H, ArH), 7.18 (s, 2H, CH₂NHCO), 6.99 (t, $J=8.5$ Hz, 4H, ArH), 3.69 (s, 4H, PhCH₂S), 3.41 (m, 4H, CH₂CH₂NH), 3.15 (s, 2H, COCH₂CO), 2.55 (t, $J=6.5$ Hz, 4H, SCH₂CH₂), $^{13}\text{C NMR}$ (100 MHz, CDCl_3) 167.3 (COCH₂CO), 162.1 ($J_{\text{CF}}=242$, FArC), 133.8 ($J_{\text{CCCCF}}=3$ Hz, ArC), 130.6 and 130.5 (d, $J_{\text{CCCF}}=8$ Hz), 115.7 and 115.5 (d, $J_{\text{CCF}}=21$ Hz), 43.1 (COCH₂CO), 38.5 (CH₂CH₂NH), 35.2 (FPhCH₂S), 30.8 (CH₂CH₂S), m/z (ESI): $[\text{M} + \text{Na}]^+$ for $[\text{C}_{21}\text{H}_{24}\text{F}_2\text{N}_2\text{NaO}_2\text{S}_2]^+$ calculated: 461.1145 found: 461.1143.

***N*¹,*N*³-bis(2-((4-nitrobenzyl)thio)ethyl)propanediamide (1h)** Yellow solid. Yield: 1.22 g (34%), m.p.: 82–85 °C., $\nu(\text{cm}^{-1})$: 3294 (N–H stretch), 1647 (amide C=O bend), 1544 and 1367 (N–O stretch), $^1\text{H NMR}$ (300 MHz, CDCl_3) δ 8.17 (d, $J=8.5$ Hz, 4H, ArH), 7.50 (d, $J=8.5$ Hz, 4H, ArH), 7.19 (s, 2H, CH₂CH₂NH), 3.80 (s, 4H, PhCH₂S), 3.43 (m, 4H, CH₂CH₂NH), 3.16 (s, 2H, COCH₂CO), 2.58 (t, $J=6.5$ Hz, 4H, SCH₂CH₂), $^{13}\text{C NMR}$ (75 MHz, CDCl_3) δ 167.3, (COCH₂), 147.2 (ArC), 145.9 (ArC), 129.9 (ArC), 124.0 (ArC), 42.9 (COCH₂), 38.4 (CH₂CH₂NH), 35.4

(PhCH₂S), 31.0 (SCH₂CH₂), m/z (ESI): $[\text{M} + \text{Na}]^+$ for $[\text{C}_{21}\text{H}_{24}\text{N}_4\text{NaO}_6\text{S}_2]^+$ calculated: 515.1035, found: 515.1029.

***N*¹,*N*³-bis(2-(benzylthio)-2-methylpropyl)propanediamide (1i)** Cream solid. Yield: 0.68 g (89%), m.p.: 71–74 °C., $\nu(\text{cm}^{-1})$: 3260 (amide N–H stretch), 1663 (amide C=O bend), $^1\text{H NMR}$ (300 MHz, CDCl_3) δ 7.40–7.20 (m, 10H, ArH), 7.01 (s, 2H, CH₂NHCO), 3.71 (s, 4H, PhCH₂S), 3.32 (d, $J=6.0$ Hz, 4H, C(CH₃)₂CH₂NH), 3.11 (s, 2H, COCH₂CO), 1.29 (s, 12H, SC(CH₃)₂CH₂), $^{13}\text{C NMR}$ (75 MHz, CDCl_3) δ 167.3 (NHCOCH₂), 138.3 129.0, 128.8 and 127.2 (ArC), 48.0 (CH₂NHCO), 46.6 (PhCH₂S), 43.2 (COCH₂CO), 33.1 (SC(CH₃)₂), 26.8 (SC(CH₃)₂), m/z (ESI): $[\text{M} + \text{Na}]^+$ for $[\text{C}_{25}\text{H}_{34}\text{N}_2\text{NaO}_2\text{S}_2]^+$ calculated: 481.1959 found: 481.1959.

General synthesis procedure for the *N*¹,*N*³-bis(2-(benzylthio)ethyl) diethylpropanediamide derivatives (3a–e)

To a stirred solution of amine **2a–e** (1 eq.) and triethylamine (1 eq.) in dry diethyl ether was added a dry diethyl ether solution of diethyl malonyl chloride (0.5 eq.) dropwise for 90 min. The reaction mixture was left to stir overnight after which H₂O was added, and the crude product was extracted using diethyl ether. The diethyl extract was washed successively with HCl (2 M), NaHCO₃, H₂O and brine after which it was dried over Na₂SO₄ and concentrated in vacuo. The crude product was purified by flash chromatography (20% EtOAc/Hexane to 100% EtOAc) to give the diethylpropanediamide derivatives **3a–e**.

***N*¹,*N*³-Bis(2-(benzylthio)ethyl)-2,2-diethylpropanediamide (3a)** Viscous colorless oil. Yield: 1.1 g (54%), $\nu(\text{cm}^{-1})$: 3326 (amide N–H stretch), 1630 (amide C=O bend), $^1\text{H NMR}$ (300 MHz, CDCl_3) δ 7.42 (s, 2H, CONHCH₂), 7.38–7.12 (m, 10H, ArH), 3.72 (s, 4H, SCH₂Ph), 3.41 (m, 4H, NHCH₂CH₂), 2.57 (t, $J=6.5$ Hz, 4H, CH₂CH₂S), 1.85 (q, $J=7.0$ Hz, 4H, CCH₂CH₃), 0.82 (t, $J=7.0$ Hz, 6H, CCH₂CH₃), $^{13}\text{C NMR}$ (75 MHz, CDCl_3) δ 173.2 (COC(CH₂CH₃)₂CO), 138.2, 129.0, 128.7 and 127.3 (ArC), 58.3 (COC(C₂H₅)CO), 38.2 (NHCH₂CH₂S), 35.9 (CH₂CH₂S), 31.1 (SCH₂Ph), 30.3 CCH₂CH₃), 9.6 (CCH₂CH₃). m/z (ESI): $[\text{M} + \text{H}]^+$ for $[\text{C}_{29}\text{H}_{35}\text{N}_2\text{O}_2\text{S}_2]^+$ calculated: 459.2140 found: 459.2138.

***N*¹,*N*³-Bis(2-((4-vinylbenzyl)thio)ethyl)-2,2-diethylpropanediamide (3b)** Colorless gel. Yield: 0.12 g, (83%), $\nu(\text{cm}^{-1})$: 3323 (amide N–H stretch), 1655 (amide C=O bend), $^1\text{H NMR}$ (300 MHz, CDCl_3) δ 7.36 (d, $J=7.5$ Hz, 4H, ArH and CH₂NHCO), 7.27 (d, $J=7.5$ Hz, 4H, ArH), 6.69 (dd, $J=17.5, 11$ Hz, 2H, CH₂CH₂Ph), 5.73 (d, $J=17.5$ Hz, 2H, CH₂CH₂CHPh), 5.23 (d, $J=11.0$ Hz, 2H, CH₂CH₂CHPh),

3.71 (s, 4H, CH₂CHPhCH₂S), 3.43 (m, 4H, CH₂CH₂NH), 2.57 (t, *J* = 6.5 Hz, 4H, SCH₂CH₂), 1.85 (q, *J* = 7.5 Hz, 4H, COC(CH₂CH₃)₂), 0.82 (t, *J* = 7.5 Hz, 6H, COC(CH₂CH₃)₂), ¹³C NMR (75 MHz, CDCl₃) δ 173.2 (COC(CH₂CH₃)₂CO), 137.8 and 136.7 (ArC), 136.5 (CH₂CHPh), 129.2 and 126.6 (ArC), 114.0 (CH₂CHPh), 58.3 (COC(CH₂CH₃)₂), 38.2 (CONHCH₂), 35.6 (CH₂CHPhCH₂S), 31.1 (C(CH₂CH₃)₂), 30.3 (SCH₂CH₂), 9.6 (C(CH₂CH₃)₂), *m/z* (ESI): [M + H]⁺ for [C₂₉H₃₆N₂O₂S₂]⁺ calculated: 511.2453 found: 511.2450.

N¹,N³-Bis(2-((4-methoxybenzyl)thio)ethyl)-2,2-diethylpropanediamide (3c) Viscous colorless oil. Yield: 1.27 g (45%), *v* (cm⁻¹): 3337 (NH), 1650 (amide C=O bend), 1240 (C–O; aromatic ether), ¹H NMR (300 MHz, CDCl₃) δ 7.44 (s, 2H, CH₂CH₂NH), 7.23 (d, *J* = 8.5 Hz, 4H, ArH), 6.84 (d, *J* = 8.5 Hz, 4H, ArH), 3.79 (s, 6H, CH₃O), 3.68 (s, 4H, PhCH₂S), 3.42 (m, 4H, CH₂CH₂NH), 2.56 (t, *J* = 6.5 Hz, 4H, SCH₂CH₂), 1.86 (q, *J* = 7.5 Hz, 4H, CCH₂CH₃), 0.83 (t, *J* = 7.5 Hz, 6H, CCH₂CH₃), ¹³C NMR (75 MHz, CDCl₃) δ 173.2 (NHCO), 158.8 (ArC), 130.1 (ArC), 130.0 (ArC), 114.1 (ArC), 58.3 (COCCO), 55.4 (OCH₃), 38.2 (NHCH₂CH₂), 35.3 (SCH₂Ph), 31.0 (CCH₂CH₃), 30.2 (CH₂CH₂S), 9.5 (CCH₂CH₃), *m/z* (ESI): [M + Na]⁺ for [C₂₇H₃₈N₂NaO₄S₂]⁺ calculated: 518.2171, found: 541.2165.

N¹,N³-Bis(2-((4-fluorobenzyl)thio)ethyl)-2,2-diethylpropanediamide (3d) Viscous yellow oil. Yield: 0.91 g (46%), *v*(cm⁻¹): 3296 (amide N–H), 1647 (amide C=O bend), ¹H NMR (300 MHz, CDCl₃) δ 7.42 (s, 2H, CH₂NHCO), 7.29 (t, *J* = 8.0 Hz, 4H, ArH), 7.00 (t, *J* = 8.0 Hz, 4H, ArH), 3.70 (s, 4H, SCH₂Ph), 3.44 (m, 4H, NHCH₂CH₂), 2.56 (t, *J* = 6.0 Hz, 4H, CH₂CH₂S), 1.87 (q, *J* = 7.0 Hz, 4H, CCH₂CH₃), 0.83 (t, *J* = 7.0 Hz, 6H, CCH₂CH₃). ¹³C NMR (75 MHz, CDCl₃) δ 173.2 (COCCO), 162.1 (d, *J*_{CF} = 242, ArC), 133.9 (d, *J*_{CCCF} = 3 Hz, ArC), 130.5 (d, *J*_{CCCF} = 8 Hz), 115.6 (d, *J*_{CCF} = 21 Hz), 58.3 (COCCO), 38.2 (NHCH₂CH₂), 35.1 (SCH₂ArC), 31.1 (CCH₂CH₃), 30.3 (CH₂CH₂S), 9.6 (CCH₂CH₃). *m/z* (ESI): [M + Na]⁺ for [C₂₅H₃₂F₂N₂NaO₂S₂]⁺ calculated; 517.1771 found; 517.1765.

N¹,N³-2,2-Diethyl-bis(2-((4-nitrobenzyl)thio)ethyl)propanediamide (3e) Viscous yellow oil. Yield: 2.84 g (76%), *v*(cm⁻¹): 3294 (N–H stretch), 1647 (amide C=O bend), 1544 and 1367 (N–O stretch), ¹H NMR (300 MHz, CDCl₃) δ 8.18 (d, *J* = 8.5 Hz, 4H, ArH), 7.51 (d, *J* = 8.5 Hz, 4H, ArH), 7.45 (s, 2H, CH₂CH₂NH), 3.81 (s, 4H, PhCH₂S), 3.46 (m, 4H, SCH₂CH₂), 2.57 (t, *J* = 6.5 Hz, 4H, SCH₂CH₂), 1.87 (q, *J* = 7.5 Hz, 4H, CCH₂CH₃), 0.83 (t, *J* = 7.5 Hz, 6H, CCH₂CH₃), ¹³C NMR (75 MHz, CDCl₃) δ 173.3 (NHCO), 147.2 (ArC), 146.0 (ArC), 130.0 (ArC), 124.0 (ArC), 58.3 (COCCO), 38.2 (CH₂CH₂NH), 35.3 (PhCH₂S), 31.3 (CCH₂CH₃), 30.5 (SCH₂CH₂), 9.6 (CCH₂CH₃), *m/z* (ESI): [M + Na]⁺ for [C₂₅H₃₂N₄NaO₆S₂]⁺ calculated: 571.1661, found 571.1605.

Synthesis of silver complexes of N¹,N³-bis(2-(benzylthio)ethyl)propanediamide ([Ag(1a)]OSO₂CF₃)

The Ag⁺-**1a** complexes (**4a–c**) were accessed following the method reported by Daubinet (2001). Briefly, **1a** (1 eq.) was dissolved in EtOAc (5 mL) and added to AgOSO₂CF₃ (1, 2 or 3 eq.) also in EtOAc (5 mL) and the mixture was reacted under refluxing conditions for 15 min. The product was concentrated in vacuo and samples suitable for mass spectrometry analysis were prepared.

Silver N¹,N³-bis(2-(benzylthio)ethyl)propanediamide triflate (4a) Brown paste. Yield: 30 mg (91%), *m/z* (ESI): [M + Ag]⁺ calculated for [C₂₁H₂₆AgN₂O₂S₂]⁺; 509.0487 found; 509.0481.

Silver N¹,N³-bis(2-(benzylthio)ethyl)propanediamide triflate (4b) Brown solid. Yield: 30 mg (65%), *m/z* (ESI): [M + Ag]⁺ calculated for [C₂₁H₂₆AgN₂O₂S₂]⁺; 509.0487 found; 509.0481.

Silver (N¹,N³-bis(2-(benzylthio)ethyl)propanediamide triflate (4c) Yellow paste. Yield: 50 mg (85%). *m/z* (ESI): [M + Ag]⁺ calculated for [C₂₁H₂₆AgN₂O₂S₂]⁺; 509.0487 found; 509.0481.

Selective Ag⁺ extraction studies

The selective Ag⁺ extraction experiments were carried out following the method reported by Sole and Hiskey (1992). Briefly, a solution of equal concentrations of Cu²⁺, Ag⁺ and Pb²⁺ (4 mg/L each) in 0.023 M Na₂SO₄ and 0.476 M HNO₃ was prepared from a 500 mg/L stock solution represented the aqueous phase. The organic phase was chloroform solution of the ligands. The chloroform solvent was presaturated with twice its volume of 0.5 M H₂SO₄ by constant shaking in a separatory funnel for 5 min prior to been used to prepare the MAD ligand solutions. The concentration of the ligand solutions for each batch extraction was 1.15 M, which is equal to 250 times that of Ag⁺ (4.6 mM) used for each experiment. For each metal extraction experiment, equal volumes (10 mL) of the metal solution and the ligand solution were contacted by rapid and vigorous stirring (using a stir bar) for 15 min in a capped plastic vial partially immersed in an oil bath set at 25 °C. Each experiment was undertaken in duplicates. After stirring, the immiscible solutions were transferred to a separatory funnel, allowed to separate and collected separately. The aqueous phase was collected into a beaker and the residual chloroform was removed over a steam bath in about 15 min. Then the aqueous phase was made back up to 10 mL and prepared for ICP-OES analysis. The metal extraction efficiencies were determined using the equation:

$$\%EE = \frac{C_i - C_f}{C_i} \times 100,$$

where % EE is the percentage extraction efficiency, C_i and C_f are the initial and final metal ion concentrations, respectively.

The selectivity of the ligands for Ag^+ relative to Cu^{2+} and Pb^{2+} was determined as follows (Toure et al. 2018);

$$K_{\text{Ag}^+/\text{M}^{n+}} = \frac{D_{\text{Ag}^+}}{D_{\text{M}^{n+}}},$$

where $K_{\text{Ag}^+/\text{M}^{n+}}$ represents the selectivity coefficient of Ag^+ relative to M^{n+} ($\text{M}^{n+} = \text{Cu}^{2+}$ or Pb^{2+}), $D_{\text{M}^{n+}}$ is the distribution coefficient of the metal ions between the aqueous and the organic phases defined as;

$$D_{\text{M}^{n+}} = \frac{C_i - C_f}{C_f} \times \frac{V_{\text{aq}}}{V_{\text{org}}},$$

C_i and C_f are as defined above, V_{aq} and V_{org} are the volumes of the aqueous and the organic solutions, respectively.

Job plot and ^1H NMR titration studies of the interaction of Ag^+ and N^1, N^3 -bis(2-(benzylthio)ethyl)propanediamide (**1a**) (Fielding 2000)

Standard solutions of equal concentrations (5 mM) of ligand **1a** and AgClO_4 were prepared separately in DMSO-d_6 . Varying ratios of each solution (**1a** and AgClO_4) were then taken and mixed (with the overall concentration remaining the same) to target different Ag^+ mole fractions (χ_{Ag^+}). For example, to target a $\chi_{\text{Ag}^+} = 0.1$, a 450 μL , 5 mM **1a** solution was mixed with a 50 μL , 5 mM AgClO_4 solution inside an amber-colored NMR tube. Also, to target a $\chi_{\text{Ag}^+} = 0.2$, a 400 μL , 5 mM **1a** solution was mixed with a 100 μL , 5 mM AgClO_4 solution and so on until a $\chi_{\text{Ag}^+} = 0.9$ was prepared by mixing a 50 μL , 5 mM **1a** solution with a 450 μL , 5 mM AgClO_4 solution. The ^1H NMR experiments of all mixtures and the free ligand **1a** were recorded. The plot of $\chi_{\text{1a}} \cdot \Delta\delta$ (where χ_{1a} = mole fraction of **1a** and $\Delta\delta$ = chemical shift of Ag^+ -**1a** complex minus chemical shift of free **1a**) against χ_{Ag^+} was constructed from the data generated.

For the ^1H NMR titration study, the ligand **1a** (13 mg, 0.03 mmol) was dissolved in 500 μL DMSO-d_6 and transferred into an amber-colored NMR tube. Following this, standard solution of AgClO_4 (539 mM) was made up in DMSO-d_6 and constant volume (30 μL) of the AgClO_4 solution was added to **1a** in the NMR tube to target varying $\text{Ag}^+/\text{1a}$ mole ratios ($n_{\text{Ag}^+}/n_{\text{1a}} = 0.5$ to 4.0). For example, to target a $n_{\text{Ag}^+}/n_{\text{1a}} = 0.5$, a 30 μL , 539 mM solution of the AgClO_4 solution was added using a glass syringe to the neat **1a** solution and the ^1H NMR spectrum was recorded. Also, to target a $n_{\text{Ag}^+}/n_{\text{1a}} = 1.0$, a 30 μL , 539 mM solution AgClO_4 solution was added to the AgClO_4 -**1a** solution with $n_{\text{Ag}^+}/n_{\text{1a}} = 0.5$ and the ^1H NMR spectrum was recorded. The constant addition of the AgClO_4 solution was continued until a $n_{\text{Ag}^+}/n_{\text{1a}} = 4.0$ was achieved. The plot of $\Delta\delta$ (where $\Delta\delta$ = chemical shift of Ag^+ -**1a** complex minus chemical shift of free **1a**) against $n_{\text{Ag}^+}/n_{\text{1a}}$ was constructed using the data generated.

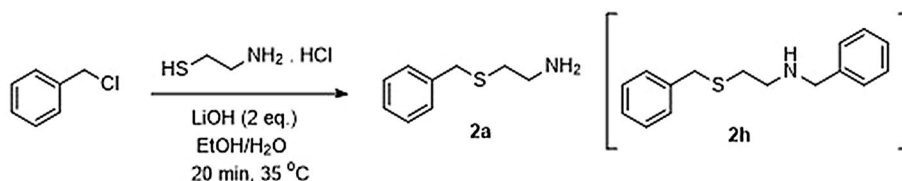
Results and discussion

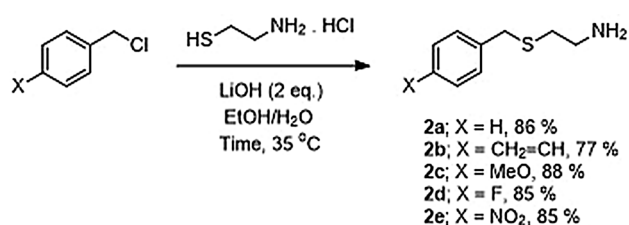
Syntheses of the 2-(benzylthio)ethan-1-amine derivatives (**2a–e**) and 2,2-dimethyl-2-benzylthioethylamine (**2g**)

The *S*-benzylcysteamines **2a–e**, which are starting materials for the synthesis of MADs **1a**, **1e–h** were accessed following a modified protocol to that reported by Ghosh and Tochtrop (2009). For the amine **2a**, it was necessary to shorten the reaction time from 40 to 20 min to minimize the formation of the dibenzylated product **2h** (Scheme 1). However, for the other amines **2b–e** it was necessary to extend the reaction time to 40 min (Scheme 2) to give good selectivity as less than 3% dibenzylated products were observed as evidenced from their ^1H NMR spectra. Using these reaction durations (20 min for **2a** and 40 min for **2b–e**), the desired compounds apart from **2d** were prepared without the need for further purification as evidenced by their ^1H NMR spectra. These amines served as starting material for the synthesis of **1a** and **1e–h**.

To assess the effect of sterics on Ag^+ efficiency and selectivity by the novel MAD ligands, the substituted *S*-benzylcysteamine **2g** was synthesized by a modification of a method reported by Carroll, White, and Wall (1963) as schematized in Scheme 3. The poor yield (23%) obtained for **2g** was attributed

Scheme 1 Illustration of the synthesis of amine **2a** showing the dibenzylated byproduct **2h**





Scheme 2 Syntheses of the 2-(benzylthio)ethan-1-amine derivatives (2a–e)

to the loss of acetone during the reaction. This amine **2g** will be employed for the synthesis of a novel MAD **1i** (Fig. 2) with steric hinderance at the α -position of the sulfur atom.

Syntheses of the *N*¹,*N*³-bis(2-(benzylthio)ethyl)propanediamide derivatives (**1a**, **1e–i** and **3a–e**)

In the original published procedure by Daubinet and Kaye (2002), access to the ligand **1a** required a reaction duration of 7 days, at the end of which a yield of 24% was obtained. We prepared **1a** in less than 1 day with an improved yield of 33% through an alternative pathway involving the drop-wise addition of one equivalent of malonyl chloride to four equivalents of the amine **2a** in dry THF (Scheme 4). Related

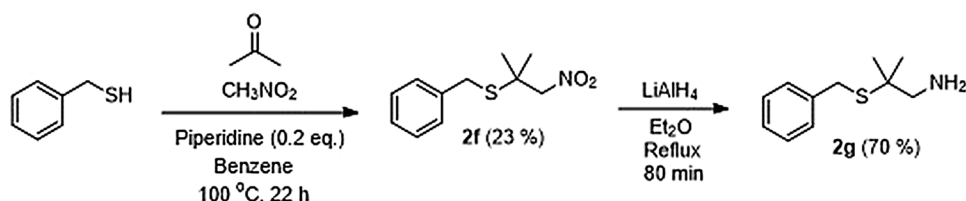
ligands **1e–i** were accessed (in low to high yields) using the same protocol (Scheme 4).

The gem-diethyl MADs **3a–e** were obtained in much better yields (46–75%) than those obtained for the unsubstituted MADs (**1a** and **1e–i**), presumably due to removal of competing enolization pathways that would lower the yields (Scheme 5).

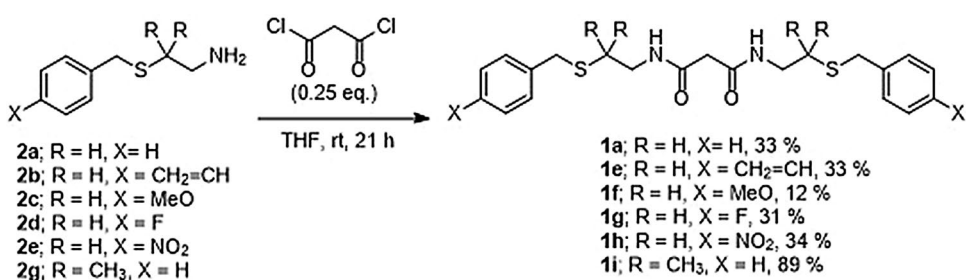
Ag⁺ extraction studies

Extraction studies in chloroform, following the method reported by Sole and Hiskey (1992), were carried out to assess the selectivity and efficiency of Ag⁺ extraction by the MAD ligands **1a**, **1e–h** and **3a** prepared. Prior to its use in preparation of the ligand solutions, the chloroform solvent was presaturated with twice its volume of an acidified deionized H₂O to remove any H₂O-soluble components to minimize volume changes during the solvent metal extraction process. We decided to prepare mixed metal aqueous solutions with very low concentrations (4 mg/L) of Ag⁺, Cu²⁺ and Pb²⁺ because Ag⁺ typically exists in very low concentrations in Ag⁺ repositories where our novel MAD ligands may be applied (Crane et al. 2017). The choice of Cu²⁺ and Pb²⁺ as competing ions for the efficiency and selectivity

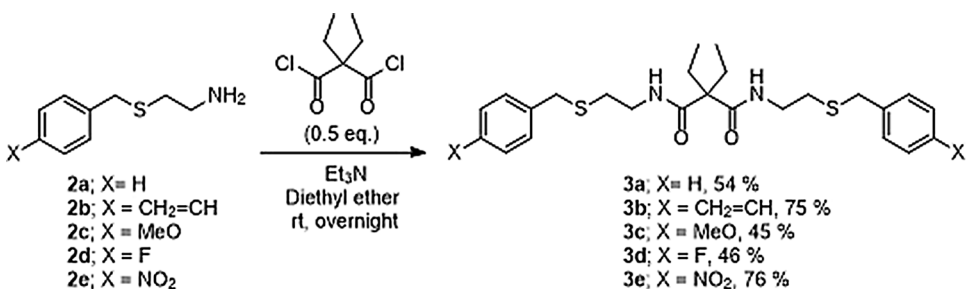
Scheme 3 Synthesis of 2,2-dimethyl-2-benzylthioethylamine (**2g**)



Scheme 4 Syntheses of the malondiamide derivatives (**1a**, **1e–i**)



Scheme 5 Syntheses of the gem-diethyl malondiamide derivatives (**3a–e**)



extractions is borne out of the knowledge that these metals usually coexist with Ag^+ in ores and mine tailings, for instance (Crane et al. 2017). For sensible comparisons to be made, each solvent extraction experiment was undertaken in duplicate and with vigorous stirring (using a stir bar with equal volumes of ligand and metal solutions for 15 min). The concentration of the metals in the raffinate was measured by means of ICP-OES and each metal concentration value was the average of three analytic runs.

A control experiment was undertaken with the metal solution using the chloroform solvent without any ligand present. This would determine any extraction efficiency of the solvent itself (the background extraction) and any possible extraction due to the plastic vials used for the experiment. Interestingly, we observed that the neat chloroform itself (the control) was able to extract some metals with a slight preference for Ag^+ (Fig. 3). This is likely due to either the differential partial solubility of these metals in chloroform or Ag^+ adsorbed onto the inner walls of the plastic vial. Notwithstanding, the extraction efficiency of the **1a** for Ag^+ was significantly higher than that in the control experiment (Fig. 3), underlining the importance of **1a** in efficient Ag^+ extraction.

Electronics effect

The effect of electronic differences in the aryl grouping of the MAD ligands on the efficiency and selectivity of Ag^+ recovery was studied by comparing extraction efficiencies and selectivity's exhibited by the ligands **1a** and **1e-h**. The observed extraction efficiencies are presented in Fig. 4. While the efficiencies for Ag^+ extraction by these ligands differ only slightly; **1a** = $(96.3 \pm 1.2)\%$, **1e** = $(98.4 \pm 0.4)\%$, **1f** = $(94.1 \pm 1.6)\%$, **1g** = $(91.1 \pm 1.0)\%$, **1h** = $(91.1 \pm 2.7)\%$ (Fig. 4) extraction efficiencies for those with electron withdrawing substituents **1g** and **1h** are the lowest (extraction efficiency order: **1h** = **1g** < **1f** < **1a** < **1e**) (Table 1).

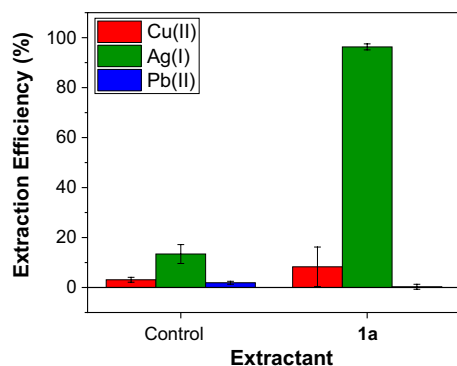


Fig. 3 ICP-OES data showing metal extraction efficiencies in the control and the malondiamide-derived ligand **1a** ($[\text{M}^{n+}] = 4$ mg/L each, volume of organic and aqueous phases = 10 mL each, contact time = 15 min)

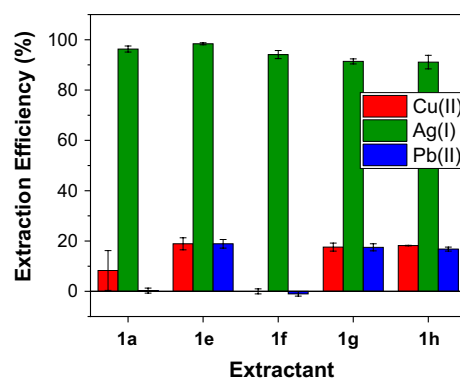


Fig. 4 ICP-OES data showing metal extraction efficiencies by the malondiamide-derived ligands **1a**, **1e-h** ($[\text{M}^{n+}] = 4$ mg/L each, volume of organic and aqueous phases = 10 mL each, contact time = 15 min)

The highest extraction efficiency observed for **1e** could be because it would give the least polar Ag^+ complex and thus have the highest solubility in chloroform (Ocak et al. 2006). Correspondingly, the least extraction efficiencies were observed for **1g** ($\text{X} = \text{F}$) and **1h** ($\text{X} = \text{NO}_2$) because (a) the Ag^+ complexes are the most polar and so less soluble in chloroform (Ocak et al. 2006) and (b) the electron withdrawing nature of the aryl groups may have made the sulfur donor atom lone pairs less available for binding Ag^+ (the soft sulfur atom being crucial in efficiency and selectivity following the HSAB rule) (Pearson 1968). For the methoxy analogue **1f**, a combination of the polar nature of the Ag^+ -**1f** complex lowering extraction efficiency with the electron donation activity of the methoxy group making the sulfur atom lone pairs readily available and increasing the binding to Ag^+ leads to an intermediate extraction efficacy. The latter explanation (b), if true, would also explain the poorer selectivity's of the ligands with electron withdrawing groups (**1e**, **1g**, **1h**), noting that in the styryl analogue **1e** the inductive electron withdrawing nature of the vinyl group will be the dominant effect. A greater selectivity would be predicted and is observed for the strongly electron donating methoxy substituent in **1f**, where selectivity for Ag^+ versus Cu^{2+} is approximately nine times better than was observed by **1a**.

Table 1 Efficiency and selectivity of malondiamide-derived ligands **1a**, **1e-h** for Ag^+ relative to Cu^{2+} and Pb^{2+}

Ligand	Efficiency (%)	$K_{\text{Ag}^+/\text{Cu}^{2+}}$	$K_{\text{Ag}^+/\text{Pb}^{2+}}$
1a	96.3 ± 1.2	11.6	321
1e	98.4 ± 0.4	5.2	5.2
1f	94.1 ± 1.6	85.5	235.3
1g	91.1 ± 1.0	5.2	5.2
1h	91.1 ± 2.7	5.0	5.4

The results observed here suggest that electronics have only a small influence on the efficiency of Ag^+ extraction by these ligands but a significant effect on selectivity. The implication of this result for large scale Ag^+ recovery is that purer Ag^+ may be recovered from a mixed metal solution by a ligand bearing electron donating groups like the methoxy group.

Steric effect

The effect of steric hindrance at various sites in the MAD ligands was investigated. Steric hindrance around the crucial sulfur atom required for binding in ligand **1i** might be predicted to lead to lower efficiencies in Ag^+ extraction while placing steric hindrance further away at the central carbon represented by ligand **3a**, might be predicted to have less effect on the extraction of Ag^+ (Fig. 5). Ligand **1i**, sterically hindered near the sulfur atom, extracted with lesser efficiency ($\sim 4\%$) for Ag^+ ($92.2 \pm 0.2\%$) than the analogue without such steric hindrance **1a** ($96.3 \pm 1.2\%$), (Fig. 5) as predicted. This is attributed to the slightly greater difficulty of **1i** in assuming the right conformation needed to bind Ag^+ because of the presence of the dimethyl substitution at the α -position to the crucial sulfur donor center (Hiruta et al. 2014). On the other hand, MAD **3a**, sterically hindered at the acyl region extracted slightly higher amounts of Ag^+ compared to **1a** attributed to the higher solubility of the Ag^+ -**3a** complex in chloroform than the Ag^+ -**1a** complex [**1a** = ($96.3 \pm 1.2\%$) versus **3a** = ($98.9 \pm 0.2\%$)]. It is worth noting that the ligand **3a** extracted slightly higher amounts of Ag^+ than the ligand **1i**, attributed to the location of steric hindrance away from the crucial sulfur donor center as earlier explained. Interestingly both **1i** and **3a** were less selective than **1a** for binding Ag^+ over Pb^{2+} (**1i** $K_{\text{Ag}^+/\text{Pb}^{2+}} = 4.5$, **3a** $K_{\text{Ag}^+/\text{Pb}^{2+}} = 11.1$, **1a** $K_{\text{Ag}^+/\text{Pb}^{2+}} = 321$) and this could be attributed to the higher solubility of the Pb^{2+} complexes of **1i** and **3a**

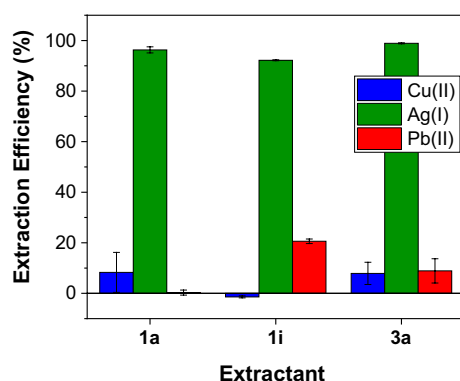


Fig. 5 ICP-OES data showing metal extraction efficiencies by malon-diamide-derived ligands **1a**, **1i** and **3a** ($[\text{M}^{n+}] = 4 \text{ mg/L}$ each, volume of organic and aqueous phases = 10 mL each, contact time = 15 min)

than that of **1a** in chloroform due to the gem dialkyl groupings (Ocak et al. 2006). Overall, steric hindrance imparted by dimethyl substitution at α -positions to the crucial sulfur donor reduced efficiency of Ag^+ extracted compared to a ligand without such hindrance. The ligand with steric hindrance occasioned by diethyl substitution at the acyl position (not in the neighborhood of the sulfur donor), was observed to demonstrate higher efficiency for Ag^+ than a ligand without such steric hindrance. Selectivity for Ag^+ against Pb^{2+} reduced in ligands with steric hindrances afforded by either dimethyl or diethyl substitutions when compared to the ligand without any steric hindrance.

Investigation of Ag^+ -**1a** binding stoichiometry

Mass spectrometry studies To gain insight into the nature of the binding of Ag^+ by the MAD ligands, the MAD **1a** was chosen as a case study. This is because **1a** contains only the basic motif reported to be responsible for Ag^+ binding (Daubinet 2001). Therefore, Ag^+ complexes of **1a**, were prepared by varying the equivalents of the silver salt (1–3 eq.) relative to the ligand **1a** (Table 2). Consequently, the Ag^+ -**1a** complexes (**4a–c**) were obtained in moderate to high yields (Table 2) and characterized by means of low- and high-resolution mass spectrometry. In the wide scan (m/z 0–2400) low resolution mass spectrometry (LRMS) of **4a**, the only pair of peaks with ratio of $\sim 1:1$ (indicative of a Ag^+ complex) were observed at m/z 509 and 511 (Fig. 6). Indeed, the m/z 509 was confirmed by high resolution mass spectrometry (HRMS) analyses as the complex— $[\text{}^{107}\text{Ag}(\mathbf{1a})]^+$ (found: 509.0481, calculated: 509.0487). Interestingly, reacting the ligand **1a** with two equivalents and three equivalents of silver triflate gave **4b** and **4c**, respectively (Table 2, entries 2 and 3) which were also both found, after LRMS analyses, to be Ag^+ -**1a** complexes with a 1:1 stoichiometry. These results indicate that the binding stoichiometry of the Ag^+ complex with MAD **1a** is perhaps 1:1.

Table 2 Effect of Ag^+ equivalent on stoichiometry of $\text{AgOSO}_2\text{CF}_3$ -**1a** complexes **1a** $\xrightarrow[\text{EtOAC, Reflux, 15 min}]{1-3 \text{ eq.}}$ $[\text{Ag}_x(\mathbf{1a})_y]^{n+}$

Entry	Ligand	AgO- SO_2CF_3 eq	Product	$\text{Ag}^+:\mathbf{1a}$	Yield (%)
1	1a	1	4a	1:1	91
2	1a	2	4b	1:1	65
3	1a	3	4c	1:1	85

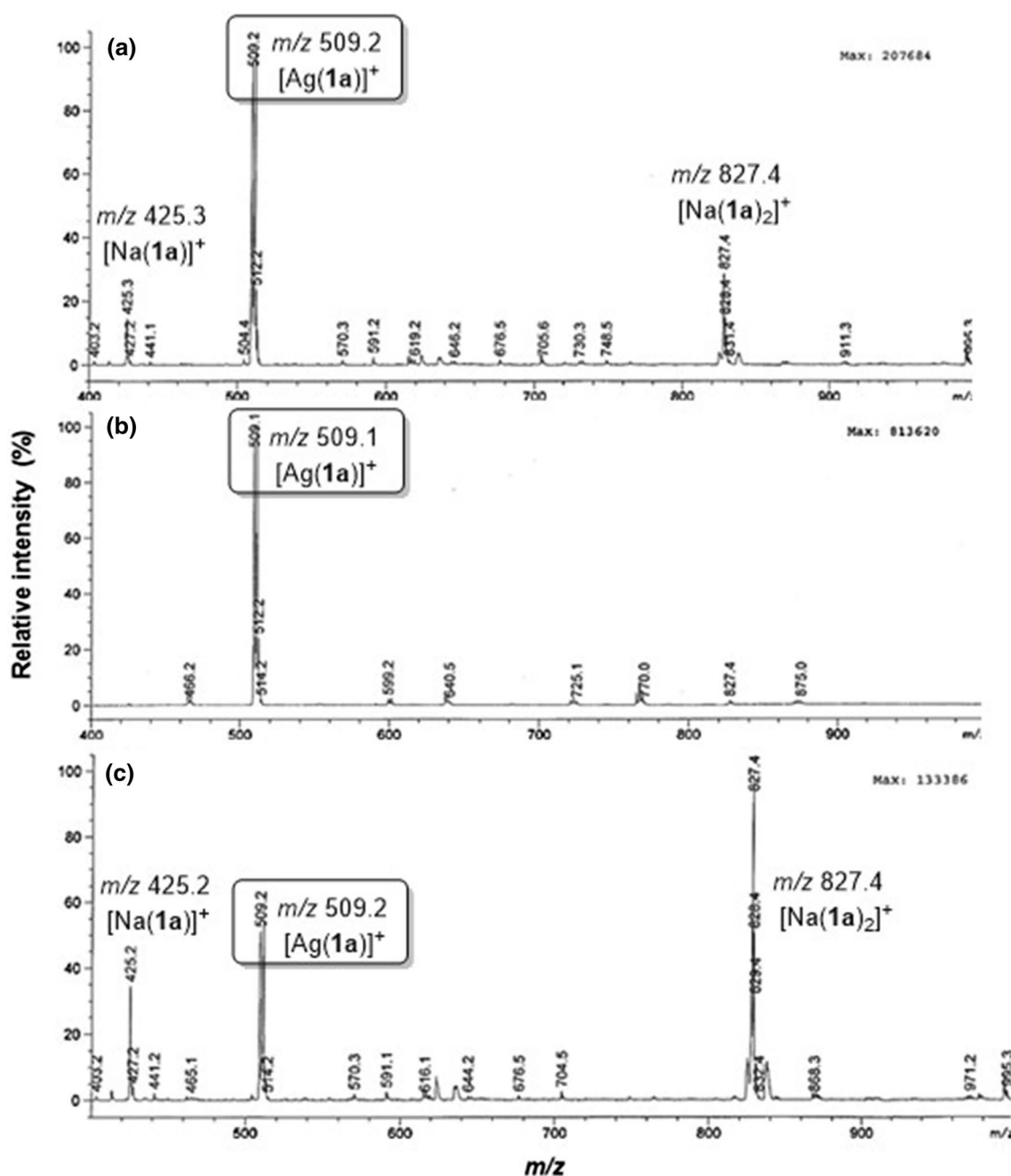


Fig. 6 Partial low-resolution ESI mass spectra of $\text{Ag}^+\text{-1a}$ complexes from treatment of **1a** with (a) one (b) two and (c) three equivalents of Ag^+

Job plot and ^1H NMR titration studies

The Job plot study for the $\text{Ag}^+\text{-1a}$ complex was carried out using equal concentrations (5 mM) of ligand **1a** and AgClO_4 in DMSO-d_6 after initial solvent screening experiments revealed the unsuitability of other common NMR solvents tested (due to poor solubility of the ligand **1a**). The Job plot experiment did not lead to the appearance of new peaks (Fig. 7a) but caused distinct changes in chemical shifts, indicating a fast rate of Ag^+ exchange between the complexed and

uncomplexed states. The gentle curvature of the curves in the Job plot (Fig. 7b) indicates the binding between the ligand **1a** and Ag^+ is perhaps weak (Swiegers and Malefetse 2000; Renny et al. 2013). Furthermore, it can be observed that the coefficient on the x-axis of the maxima of all curves in the Job plot is at $\chi_{\text{Ag}^+} = 0.5$, indicating that **1a** binds Ag^+ in any of the 1:1, 2:2 or any other $n:n$ fashion. To confirm the actual stoichiometry, ^1H NMR titration study of the interaction of **1a** with Ag^+ was carried out. Therefore, a constant amount of a 539 mM Ag^+ solution was successively added to the ligand

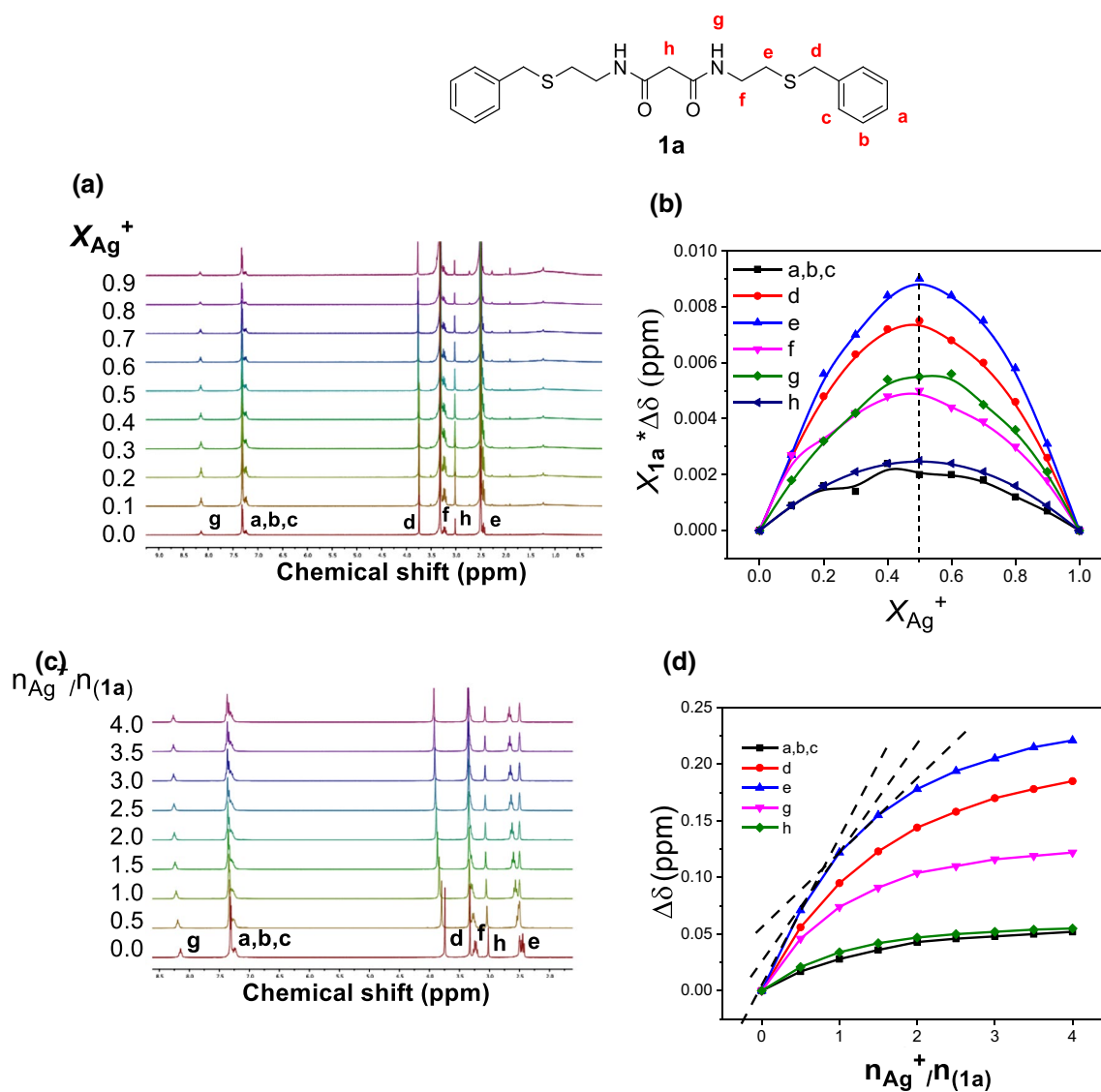


Fig. 7 (a, c) ^1H NMR (300 MHz) spectra of the interaction of Ag^+ with **1a**. (b) Job plot and (d) ^1H NMR titration plot of the interaction of Ag^+ with ligand **1a** (For job plot, $[\text{1a}] = [\text{Ag}^+] = 5 \text{ mM}$,

solvent = DMSO- d_6 . For ^1H NMR titration, $[\text{1a}] = 60 \text{ mM}$, $[\text{Ag}^+] = 539 \text{ mM}$, solvent = DMSO- d_6)

1a solution to prepare $\text{Ag}^+/\text{1a}$ mole ratios ranging from 0.5 to 4.0. Proton NMR spectra after successive addition of the Ag^+ solution was recorded (Fig. 7c), and the ^1H NMR titration plot was constructed from the values obtained (Fig. 7d). In a typical ^1H NMR titration plot, the stoichiometry of a complex is the coefficient on the x-axis of the point of inflection. In the case of the $\text{Ag}^+ \text{-1a}$ complex (Fig. 7d), it was very difficult to get a distinct point of inflection for any of the curves, indicating a weak binding between the Ag^+ and **1a** and confirming the observation from the Job plot (Renny et al. 2013). It also suggests that the $\text{Ag}^+ \text{-1a}$ complex may be adopting more than one type of stoichiometry in solution including the 1:1 observed from mass spectrometry and the Job plot.

In the Job plot (Fig. 7b), the highest $\Delta\delta$ values were observed for protons 'e' and 'd' in **1a** (the protons on α -positions to the sulfur donor atoms). The next highest $\Delta\delta$ values were observed for protons 'g' in **1a** (the amide protons). The observed high $\Delta\delta$ s may be due to deshielding effects experienced by these protons as the sulfur and nitrogen donors participate in binding Ag^+ . Unsurprisingly, lower $\Delta\delta$ values were observed for phenyl protons ('a', 'b' and 'c' in **1a**) since they are not in the neighbourhood of the sulfur and nitrogen donors (Fig. 7b). Based on these observations, it was hypothesized that the ligand **1a** binds Ag^+ using its two sulfur and nitrogen donor centers to form a tetrahedral complex (Fig. 8).

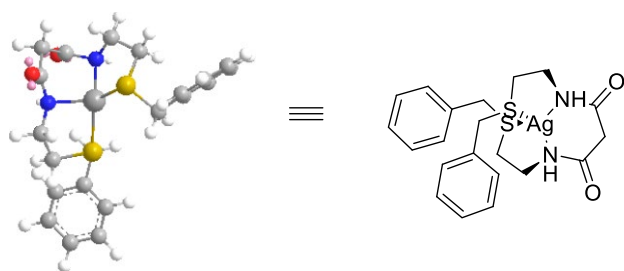


Fig. 8 Proposed optimized structure for $[\text{Ag}(\mathbf{1a})]^+$ based on stoichiometry results observed from mass spectrometry, Job plot and ^1H NMR titration results studies

Conclusion

Herein, a range of novel N^1, N^3 -bis(2-(benzylthio)ethyl)propanediamide derivatives including the divinyl derivative (**1e**) which could be attached by polymerization to a magnetic nanoparticle have been synthesized under mild conditions and in low to high yields. The effect of electronics (using **1a** and **1e–h**) and sterics (using **1a**, **1i** and **3a**) on efficiency and selectivity for Ag^+ extraction was investigated using extraction efficiencies measured following solvent extraction experiments. It was observed that electronic effects at the 4-position of the aromatic groups in the malondiamide derivatives (**1e–h**) had little effect on Ag^+ extraction efficiency but a great effect on metal selectivity, with the electron rich (4-methoxy)malondiamide derivative **1f** being the most selective and the (4-vinyl) derivative **1e** showing the best efficiency for Ag^+ over Cu^{2+} and Pb^{2+} . Increased steric hindrance at the α -positions to the sulfur donors conferred by dimethyl substitutions lowered efficiency and selectivity for Ag^+ when compared to the derivative **1a** lacking such hindrance. The derivative **3a** with steric hindrance at the methylene center provided by gem-diethyl substitution showed better efficiency but lower selectivity for Ag^+ than **1a** devoid of such steric hindrance. Binding studies carried out by means of mass spectrometry, Job plot and ^1H NMR titration reveal that the derivative **1a** binds Ag^+ in a 1:1 fashion leading to the inference that **1a** forms a tetrahedral complex with Ag^+ . Binding studies suggest that **1e**, our target for attachment by polymerization to a nanoparticle may also bind Ag^+ in the same way as **1a** since both ligands contain essentially the same donor atoms crucial for Ag^+ binding. In which case it is presumed that the polymerized version of **1e**—poly(**1e**), may lose its Ag^+ binding efficiency potentially due to the difficulty in wrapping round Ag^+ especially in the case where poly(**1e**) crosslinks between nanoparticles. In addition, since the dimethoxy derivative **1f** and the gem-diethyl derivative **3a** showed the best selectivity and efficiency respectively for Ag^+ , an ideal malondiamide-derived ligand for attachment to a magnetic nanoparticle would be one containing both the vinyl and methoxy groups on each of

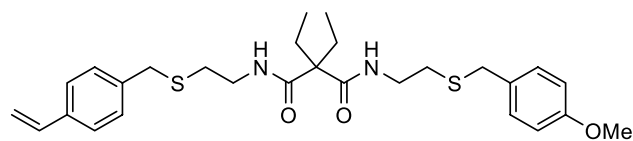


Fig. 9 Idealized structure of a highly efficient and selective N^1, N^3 -bis(2-(benzylthio)ethyl)malondiamide derivative suitable for attachment by polymerization to a magnetic nanoparticle

the 4-positions of different aromatic groups and gem-diethyl substitution at the methylene center as shown in Fig. 9.

Author contributions Conceptualization, experimental design, experimental work, first draft (ADA). Conceptualization, experimental design, paper review (AJC).

Funding The authors would like to thank The Commonwealth Scholarship Commission in the United Kingdom and The University of Warwick for funding the research under grant number NGCS-2015-448.

Data availability Not applicable.

Code availability Not applicable.

Compliance with ethical standards

Conflict of interest The authors declare no conflict of interest.

References

- Aderibigbe AD, Crane RA, Lees MR, Clark AJ (2020) Selective uptake of Ag (I) from aqueous solutions using ionic liquid-modified iron oxide nanoparticles. *J Nanoparticle Res* 216:1–14. <https://doi.org/10.1007/s11051-020-04944-1>
- Alam MS, Inoue K, Yoshizuka K, Dong Y, Zhang P (1997) Solvent extraction of silver from chloride media with some commercial sulfur-containing extractants. *Hydrometallurgy* 44:245–254. [https://doi.org/10.1016/S0304-386X\(96\)00053-9](https://doi.org/10.1016/S0304-386X(96)00053-9)
- Avarmaa K, Klemettinen L, O'Brien H, Taskinen P (2019) Urban mining of precious metals via oxidizing copper smelting. *Miner Eng* 133:95–102. <https://doi.org/10.1016/j.mineng.2019.01.006>
- Bray DJ, Clegg JK, Wenzel M, Gloe K, McMurtrie JC, Jolliffe KA, Gloe K, Lindoy LF (2015) Selective solvent extraction of silver(I) by tris-pyridyl tripodal ligands and X-ray structure of a silver(I) coordination polymer incorporating one such ligand. *Aust J Chem* 68:549–554. <https://doi.org/10.1071/CH14540>
- Carroll FI, White JD, Wall ME (1963) Organic sulfur compounds. I. Synthesis of sec-Mercaptoalkylamine Hydrochlorides 1a, b. *J Org Chem* 28:1236–1239. <https://doi.org/10.1021/jo01040a017>
- Chen C, Wang J (2008) Removal of Pb(II), Ag(I), Cs(I) and Sr(II) from aqueous solution by brewery's waste biomass. *J Hazard Mater* 151:65–70. <https://doi.org/10.1016/j.jhazmat.2007.05.046>
- Crane RA, Sinnott DE, Cleall PJ, Sapsford DJ (2017) Physicochemical composition of wastes and co-located environmental designations at legacy mine sites in the south west of England and Wales: Implications for their resource potential. *Resour Conserv Recycl* 123:117–134. <https://doi.org/10.1016/j.resconrec.2016.08.009>

- Daubinet A (2001) Design, synthesis and evaluation of silver-specific ligands. Rhodes University, Grahamstown
- Daubinet A, Kaye PT (2002) Designer ligands. VIII. Thermal and microwave-assisted synthesis of silver(I)-selective ligands. *Synth Commun* 32:3207–3217. <https://doi.org/10.1081/SCC-120013745>
- El-Shafey ESI, Al-Kindy SMZ (2013) Removal of Cu(II) and Ag(I) from aqueous solution on a chemically-carbonized sorbent from date palm leaflets. *Environ Technol (UK)* 34:395–406. <https://doi.org/10.1080/09593330.2012.698647>
- Fielding L (2000) Determination of association constants (K_a) from solution NMR data. *Tetrahedron* 56:6151–6170. [https://doi.org/10.1016/S0040-4020\(00\)00492-0](https://doi.org/10.1016/S0040-4020(00)00492-0)
- Ghosh S, Tochtrop GP (2009) A new strategy for the synthesis of β -benzylmercaptoethylamine derivatives. *Tetrahedron Lett* 50:1723–1726. <https://doi.org/10.1016/j.tetlet.2009.01.133>
- Grigorieva NA, Fleitlikh IY, Logutenko OA (2018) Silver extraction from hydrochloric acid solutions with the disulfide of bis(2,4,4-trimethylpentyl)dithiophosphinic acid. *Solvent Extr Ion Exch* 36:162–174. <https://doi.org/10.1080/07366299.2018.1446675>
- Hiruta Y, Watanabe T, Nakamura E, Iwasawa N, Sato H, Hamada K, Citterio D, Suzuki K (2014) Steric hindrance effects in tripodal ligands for extraction and back-extraction of Ag(I). *RSC Adv* 4:9791–9798. <https://doi.org/10.1039/c3ra45700a>
- Jańczewski D, Reinhoudt DN, Verboom W, Malinowska E, Pietrzak M, Hill C, Allignol C (2007) Tripodal (N-alkylated) CMP(O) and malonamide ligands: synthesis, extraction of metal ions, and potentiometric studies. *New J Chem* 31:109–120. <https://doi.org/10.1039/b613254e>
- Kolpakova N, Sabitova Z, Sachkov V, Medvedev R, Nefedov R, Orlov V (2019) Determination of Au(III) and Ag(I) in carbonaceous shales and pyrites by stripping voltammetry. *Minerals* 9:78. <https://doi.org/10.3390/min9020078>
- Manchanda VK, Pathak PN (2004) Amides and diamides as promising extractants in the back end of the nuclear fuel cycle: an overview. *Sep Purif Technol* 35:85–103. <https://doi.org/10.1016/j.seppur.2003.09.005>
- Nishihama S, Hirai T, Komasa I (2001) Review of advanced liquid-liquid extraction systems for the separation of metal ions by a combination of conversion of the metal species with chemical reaction. *Ind Eng Chem Res* 40:3085–3091. <https://doi.org/10.1021/ie010022>
- Ocak Ü, Alp H, Gökçe P, Ocak M (2006) The synthesis of new N2 S2-Macrocyclic schiff base ligands and investigation of their ion extraction capability from aqueous media. *Sep Sci Technol* 41:391–401. <https://doi.org/10.1080/01496390500496942>
- Ohto K, Yamaga H, Murakami E, Inoue K (1997) Specific extraction behavior of amide derivative of calix[4]arene for silver (I) and gold (III) ions from highly acidic chloride media. *Talanta* 44:1123–1130. [https://doi.org/10.1016/S0039-9140\(97\)00019-2](https://doi.org/10.1016/S0039-9140(97)00019-2)
- Ölmez T (2009) The optimization of Cr(VI) reduction and removal by electrocoagulation using response surface methodology. *J Hazard Mater* 162:1371–1378. <https://doi.org/10.1016/j.jhazmat.2008.06.017>
- Patil AB, Pathak PN, Shinde VS, Mohapatra PK (2014) Synthesis and evaluation of N, N'-dimethyl-N, N'-dicyclohexyl-malonamide (DMDCMA) as an extractant for actinides. *Sep Sci Technol* 49:2927–2932. <https://doi.org/10.1080/01496395.2014.943772>
- Pearson RG (1968) Hard and soft acids and bases, HSAB, part I: Fundamental principles. *J Chem Educ* 45:581–587. <https://doi.org/10.1021/ed045p581>
- Renny JS, Tomasevich LL, Tallmadge EH, Collum DB (2013) Method of continuous variations: applications of job plots to the study of molecular associations in organometallic chemistry. *Angew Chem-Int Ed* 52:11998–12013. <https://doi.org/10.1002/anie.201304157>
- Saha R, Guha S, Sahana A, Das D (2013) N, N-bis-(2-benzimidazolylmethyl)-L-methionine: an efficient Ag(I) extractant. *J Anal Chem* 68:398–402. <https://doi.org/10.1134/S1061934813050146>
- Sahan M, Kucuker MA, Demirel B, Kuchta K, Hursthouse A (2019) Determination of metal content of waste mobile phones and estimation of their recovery potential in Turkey. *Int J Environ Res Public Health* 16:887. <https://doi.org/10.3390/ijerph16050887>
- Selim KA, El HFI, Khalek MAA, Osama I (2017) Kinetics and thermodynamics of some heavy metals removal from industrial effluents through electro-flotation process. *Colloid Surf Sci* 2:47–53. <https://doi.org/10.11648/j.css.20170202.11>
- Shimojo K, Goto M (2004) Solvent extraction and stripping of silver ions in room-temperature ionic liquids containing calixarenes. *Anal Chem* 76:5039–5044. <https://doi.org/10.1021/ac049549x>
- Sole KC, Hiskey JB (1992) Solvent extraction characteristics of thio-substituted organophosphinic acid extractants. *Hydrometallurgy* 30:345–365. [https://doi.org/10.1016/0304-386X\(92\)90093-F](https://doi.org/10.1016/0304-386X(92)90093-F)
- Sun PP, Min BJ, Kim STA, Cho SY (2017) Separation of silver (I) and zinc(II) from nitrate solutions by solvent extraction with LIX63. *Mater Trans* 58:287–290. <https://doi.org/10.2320/matertrans.M2016316>
- Swiegers GF, Malefetsé TJ (2000) New self-assembled structural motifs in coordination chemistry. *Chem Rev* 100:3483–3537. <https://doi.org/10.1021/cr990110s>
- Taillades G, Sarradin J (2004) Silver: High performance anode for thin film lithium ion batteries. *J Power Sources* 125:199–205. <https://doi.org/10.1016/j.jpowsour.2003.07.004>
- Toure M, Arrachart G, Duhamet J, Pellet-Rostaing S (2018) Tantalum and niobium selective extraction by alkyl-acetophenone. *Metals (Basel)* 8:1–11. <https://doi.org/10.3390/met8090654>
- Virolainen S, Tyster M, Haapalainen M, Sainio T (2015) Ion exchange recovery of silver from concentrated base metal-chloride solutions. *Hydrometallurgy* 152:100–106. <https://doi.org/10.1016/j.hydromet.2014.12.011>
- Zanain M, Lovitt R (2013) Removal of silver from wastewater using cross flow microfiltration. *E3S Web Conf* 1:25005. <https://doi.org/10.1051/e3sconf/20130125005>

Publisher's Note Springer Nature remains neutral with regard to jurisdictional claims in published maps and institutional affiliations.

Affiliations

Abiodun D. Aderibigbe^{1,2}  · Andrew J. Clark¹

¹ Department of Chemistry, University of Warwick, Coventry CV4 7AL, UK

² Present Address: Department of Chemistry, The Federal University of Technology Akure, P.M.B. 704, Akure, Ondo State, Nigeria